

1. INTRODUCTION AND BACKGROUND

Convective storms that generate hail, lightning, and damaging winds have been identified as a formidable hazard to life and property. Even more impactful are stronger storms that generate and loft liquid-phase hydrometeors to high altitudes where freezing occurs and collisions between drops, graupel, and ice crystals lead to electrification. Condensate loading, sometimes combined with the lateral entrainment of subsaturated air in the storm middle level, initiates the convective downdraft. The subsequent melting of frozen hydrometeors and subcloud evaporation of liquid precipitation, in conjunction with precipitation loading, result in the cooling and negative buoyancy that accelerate the downdraft in the unsaturated layer. A **downburst**, in general, is defined as a **strong downdraft** that induces an outburst of damaging winds at or near the ground, and a **microburst** as a very small downburst with an outflow diameter of less than 4 km and a lifetime of less than 5 minutes. This physical process is illustrated in Figure 1.

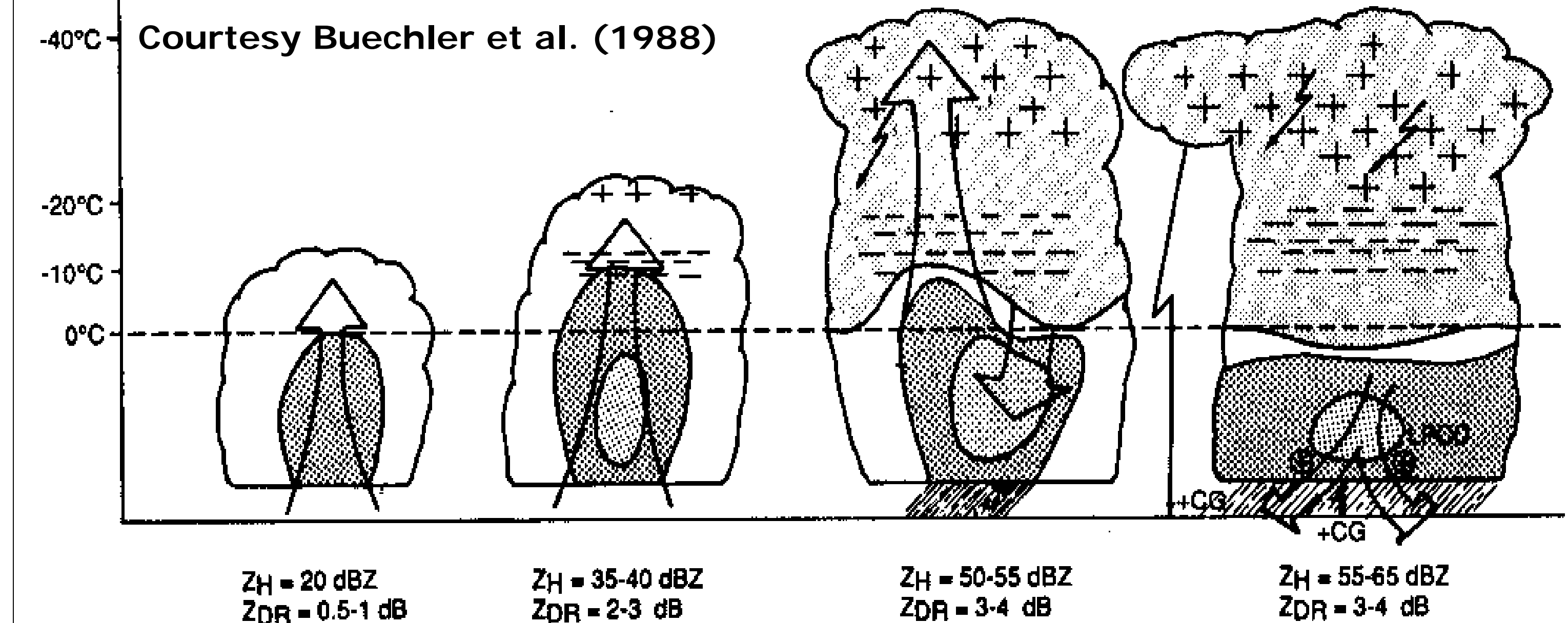
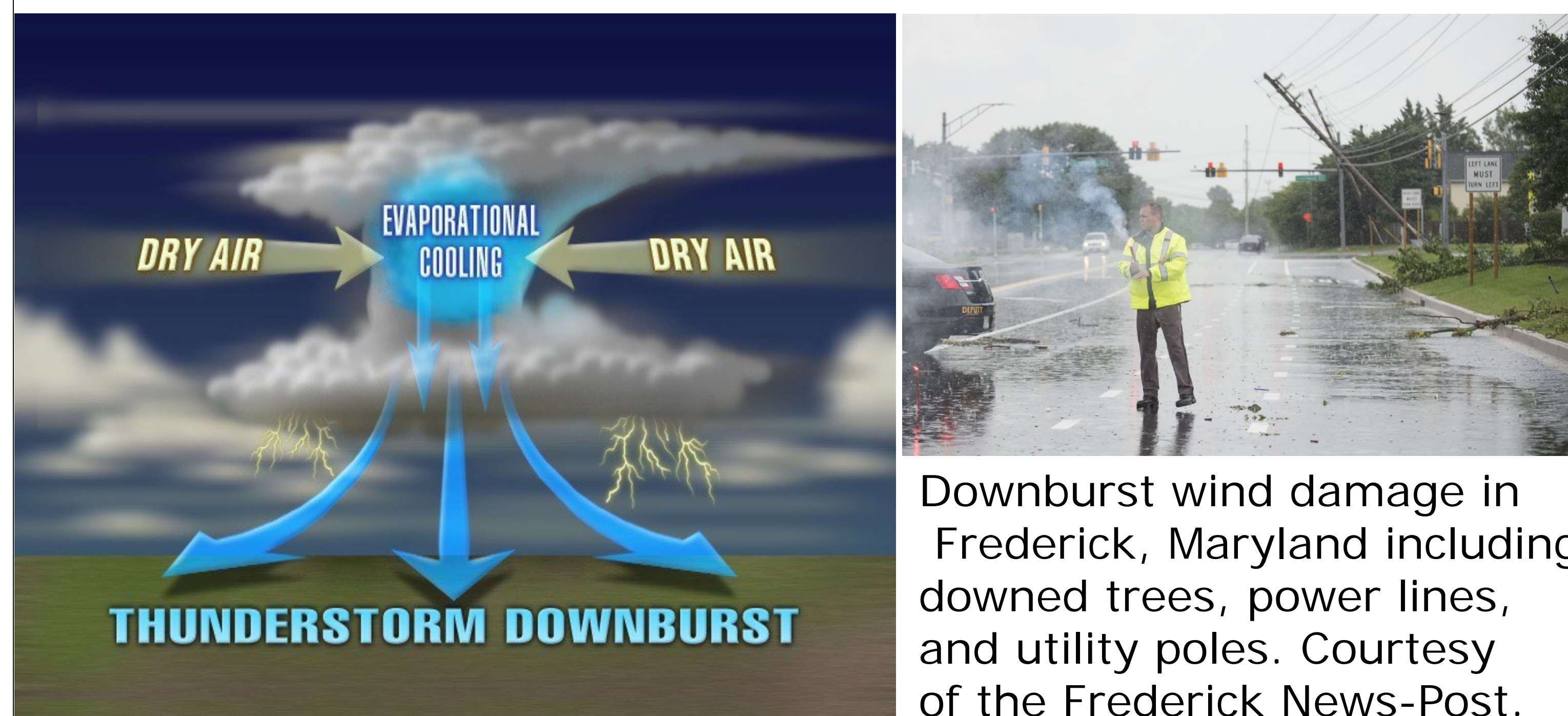


Figure 1. Conceptual model of a downburst producing thunderstorm.

2. METHODOLOGY

Selected thunderstorm events that demonstrate the physical process of downburst generation as observed simultaneously by the Geostationary Operational Environmental Satellite (GOES)-16 Advanced Baseline Imager (ABI) and Geostationary Lightning Mapper (GLM) Lightning Cluster Filter Algorithm (LCFA), Doppler radar (NEXRAD), Washington, DC Lightning Mapping Array (DCLMA), and boundary layer profilers (BLP) are analyzed. Vertical wind profile data, up to 5 km AGL, from the Cooperative Agency Profilers (CAP) system has been applied to further study the favorable environment for severe convective storm winds and the vertical structure of storm outflow. On the afternoon of **1 August 2017**, severe downburst-producing thunderstorms occurred in the United States Mid-Atlantic region and over southern California that resulted in tree damage, downed power lines, and traffic disruptions.

3. CASE STUDIES

1 August 2017 Downbursts: Frederick, Maryland

During the afternoon of 1 August 2017, a cluster of strong thunderstorms developed and tracked southeastward in a convectively unstable air mass over the Blue Ridge Mountains of Maryland. A particularly intense thunderstorm cell developed on the southern end of the cluster and produced a severe downburst in Frederick, Maryland near 1800 UTC (1400 EDT), apparent as protrusion echoes ("PE", Fig. 3). Wind damage resulting from the downburst included downed trees, power lines, and utility poles, and resulted over 3,000 Potomac Edison customers losing electricity.

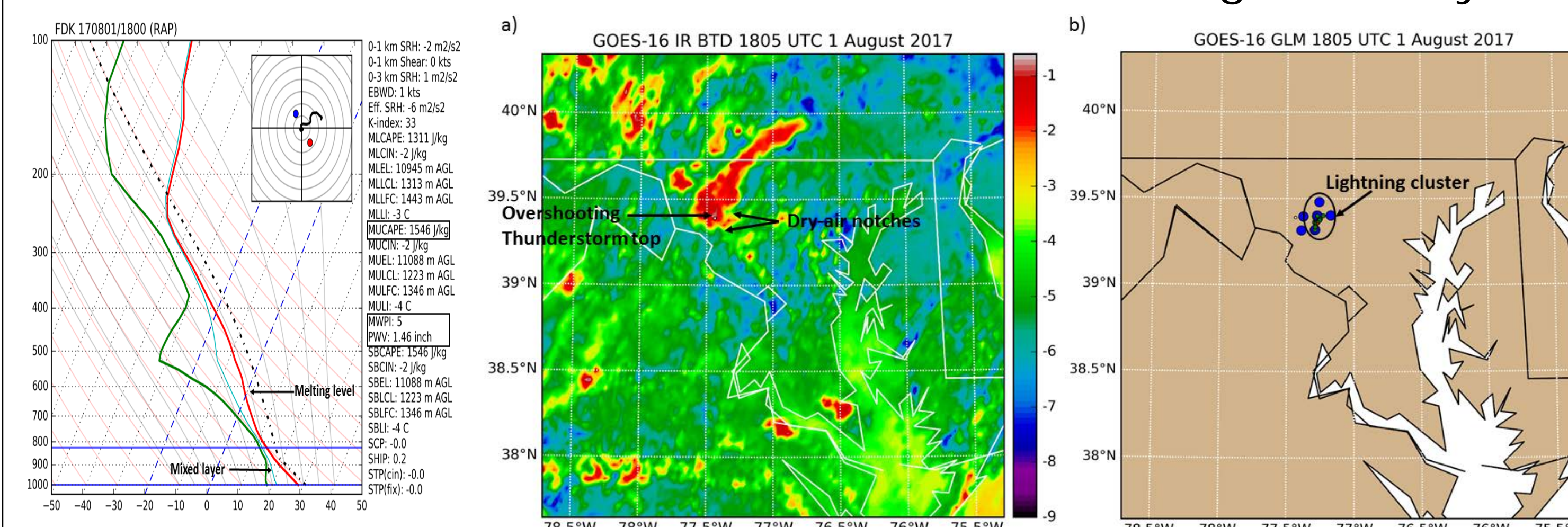


Figure 2. RAP model-derived sounding profile over Frederick (left), GOES-16 ABI Split-Window BTD (middle) and GLM LFCA product (right).

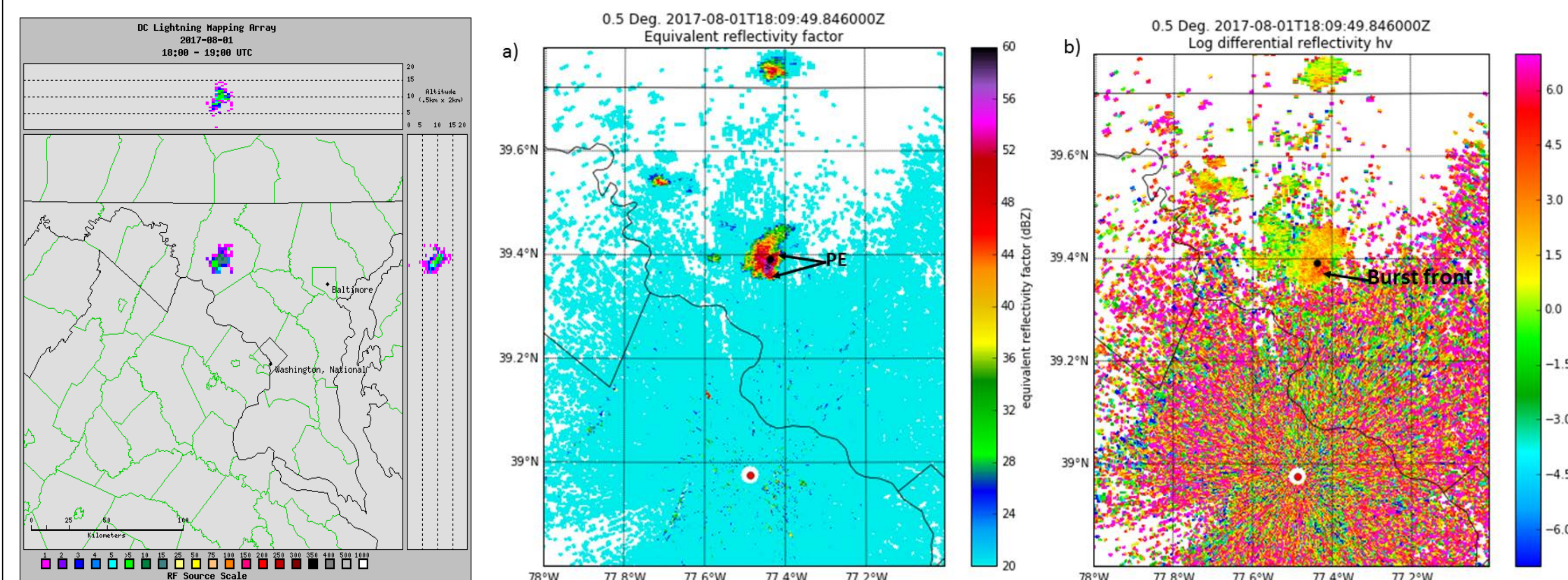


Figure 3. DCLMA lightning event image (left), Sterling, VA NEXRAD reflectivity (middle), and differential reflectivity (right) at 1809 UTC.

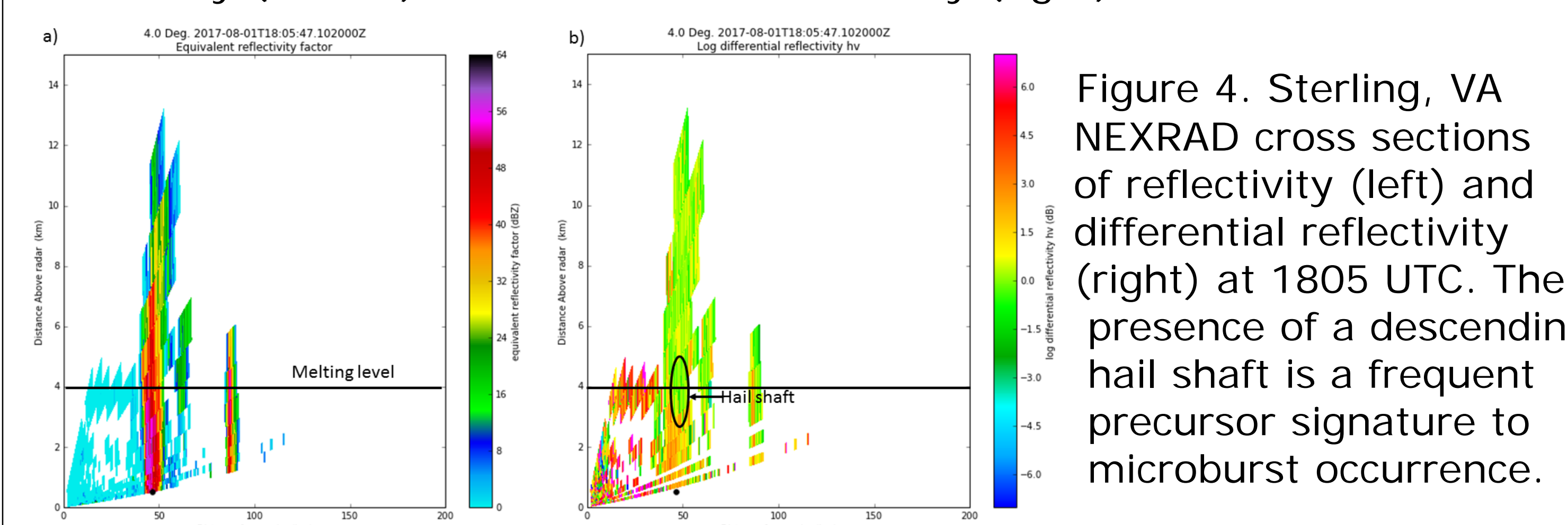


Figure 4. Sterling, VA NEXRAD cross sections of reflectivity (left) and differential reflectivity (right) at 1805 UTC. The presence of a descending hail shaft is a frequent precursor signature to microburst occurrence.

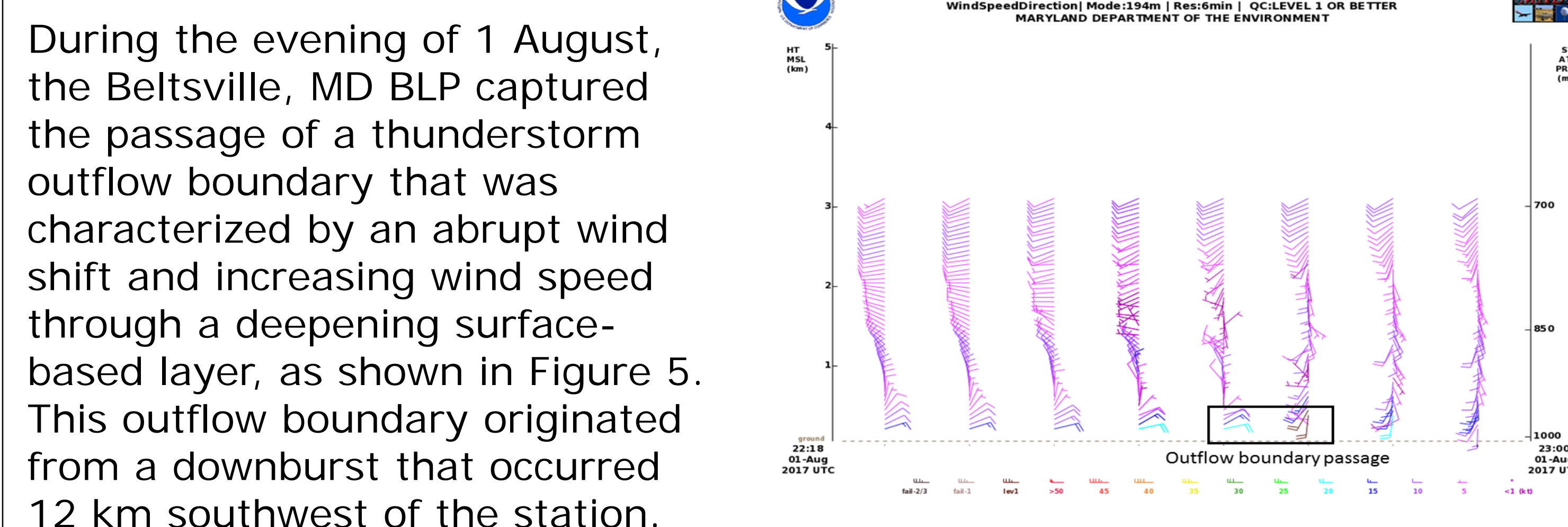


Figure 5. Beltsville, MD wind profile.

1 August 2017 Downbursts: San Diego, California

During the afternoon of 1 August 2017, a cluster of strong thunderstorms developed along the eastern boundary of the southern California marine layer and tracked northwestward over the foothills of the Laguna Mountains in San Diego County. A particularly intense thunderstorm cell developed east of San Diego and produced a strong downburst between 2020 and 2030 UTC that resulted in downed trees and traffic disruptions in the Alpine area.

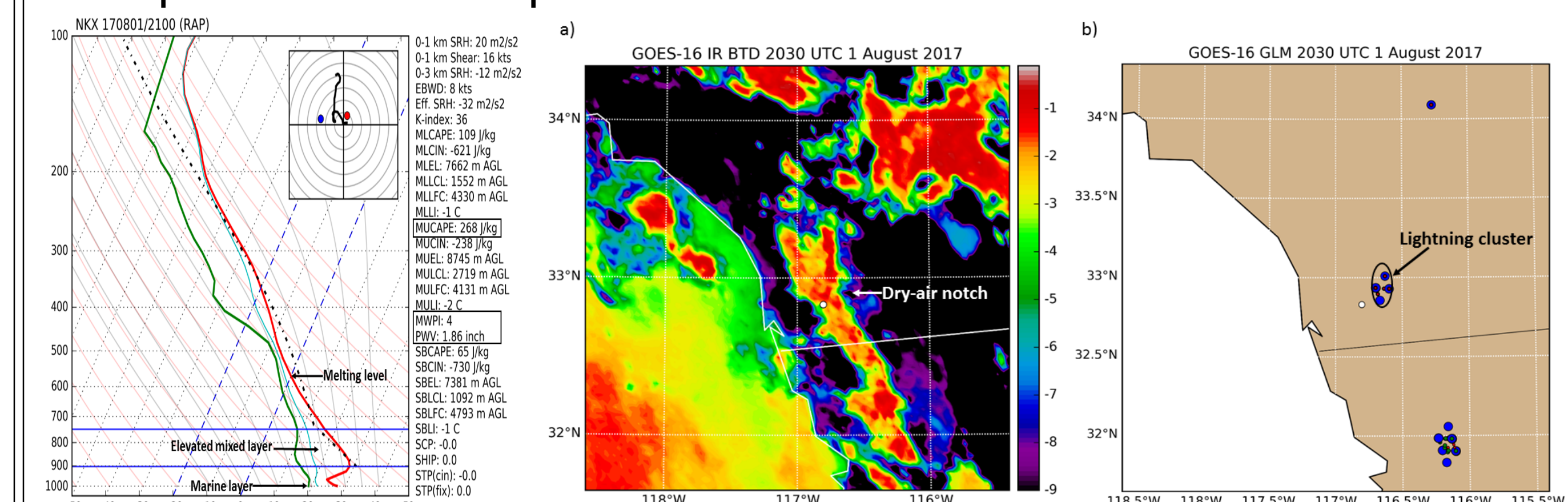


Figure 6. RAP model-derived sounding profile over San Diego (left), GOES-16 ABI Split-Window BTD (middle) and GLM LFCA product (right).

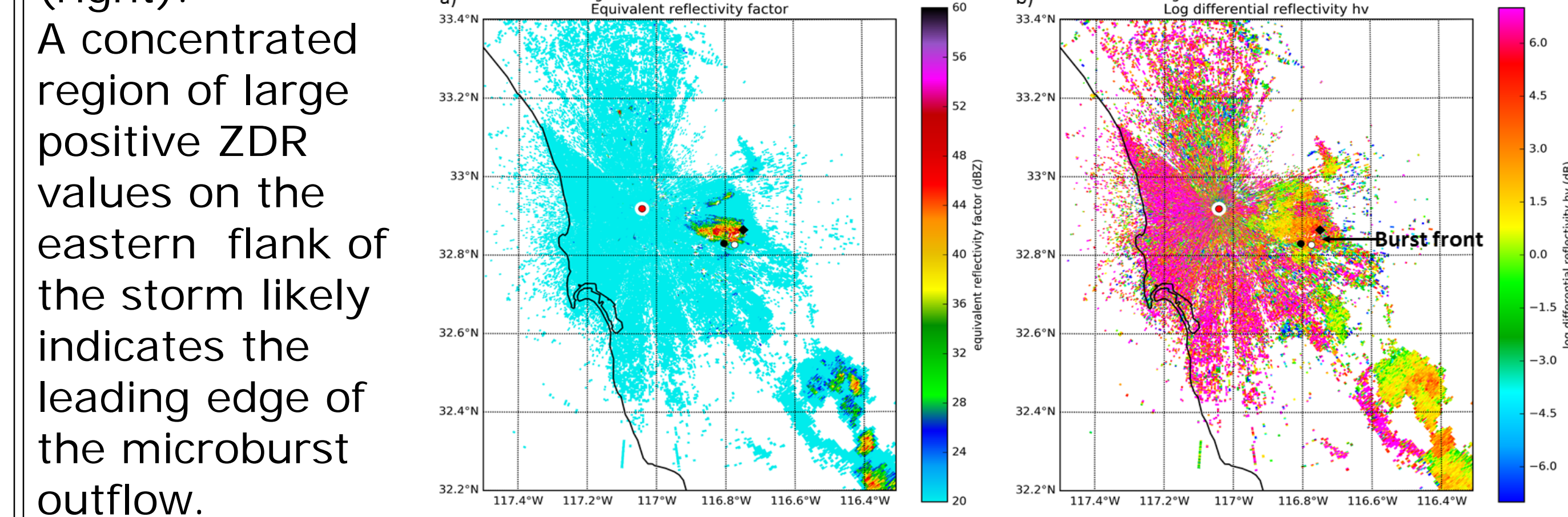


Figure 7. San Diego NEXRAD reflectivity (left), and differential reflectivity (ZDR, right) at 2031 UTC.

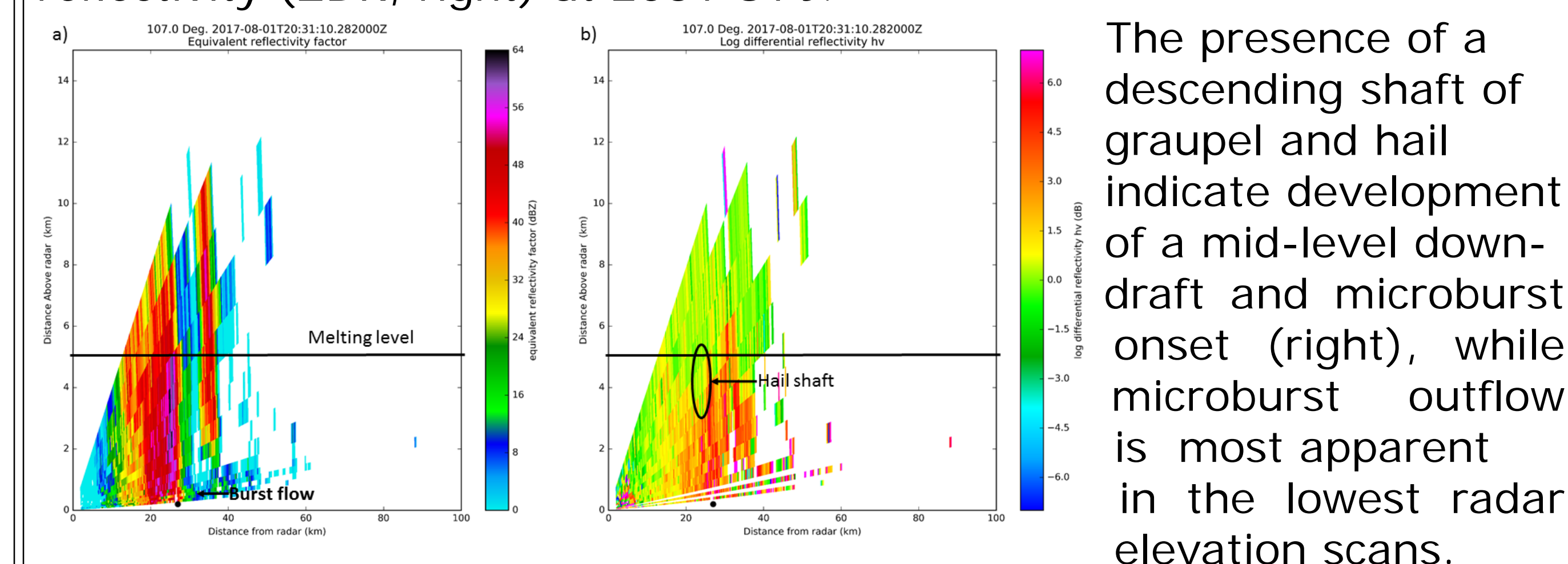


Figure 8. San Diego NEXRAD cross sections of reflectivity (left) and differential reflectivity (ZDR, right) at 2031 UTC.

4. DISCUSSION AND CONCLUSIONS

GOES-16 ABI split-window channel BTD imagery at 2-km resolution, as compared to NEXRAD imagery, displayed a high level of detail in storm structure and was effective in identifying storm-scale features, including cold cloud tops and dry-air intrusions. Corresponding GLM LFCA imagery displayed lightning events in close proximity to downburst events at the time of occurrence. DCLMA imagery verified the occurrence of lightning associated with the Frederick downburst.

References are available in paper no. 245.

Corresponding author address: Mr. Kenneth Pryor, Satellite Meteorology and Climatology Division, Operational Products Development Branch, NOAA/NESDIS/STAR, NCWCP, Rm. 2833, 5830 University Research Ct., College Park, MD 20740.

E-mail: Ken.Pryor@noaa.gov
https://www.researchgate.net/profile/Kenneth_Pryor